Pilot Study on the Feasibility of PET/CT Lymphoscintigraphy with ^{89}Zr-Nanocolloidal Albumin for Sentinel Node Identification in Oral Cancer Patients

Derrek A. Heuveling[1], Annelies van Schie[2], Danielle J. Vugts[1,2], N. Harry Hendrikse[2,3], Maqsood Yaqub[2], Otto S. Hoekstra[2], K. Hakki Karagozoglu[4], C. René Leemans[1], Guus A.M.S. van Dongen[1,2], and Remco de Bree[1]

[1]Department of Otolaryngology/Head and Neck Surgery, VU University Medical Center, Amsterdam, The Netherlands; [2]Department of Nuclear Medicine and PET Research, VU University Medical Center, Amsterdam, The Netherlands; [3]Department of Clinical Pharmacology and Pharmacy, VU University Medical Center, Amsterdam, The Netherlands; and [4]Department of Oral and Maxillofacial Surgery/Pathology, VU University Medical Center/Academic Centre for Dentistry Amsterdam, Amsterdam, The Netherlands

With conventional imaging techniques such as planar lymphoscintigraphy and SPECT/CT, preoperative sentinel node (SN) identification can be difficult when the SN is near the primary tumor, as is the case in floor-of-mouth carcinomas. PET/CT lymphoscintigraphy may improve the detection and localization of such SNs. **Methods:** In this study, the clinical feasibility of PET/CT lymphoscintigraphy using ^{89}Zr-nanocolloidal albumin was evaluated in 5 oral cancer patients. PET/CT lymphoscintigraphy was performed after peritumoral injection of ^{89}Zr-nanocolloidal albumin. The routine SN procedure, including SPECT/CT using ^{99m}Tc-nanocolloidal albumin, was performed on the same patients 7–9 d after the injection of ^{89}Zr-nanocolloidal albumin. **Results:** Comparison of radiocolloid distribution on PET/CT and SPECT/CT showed identical drainage patterns. Moreover, PET/CT was able to identify additional foci near the primary tumor. **Conclusion:** This pilot PET/CT study on SN detection indicated that lymphoscintigraphy using ^{89}Zr-nanocolloidal albumin is feasible.

Key Words: sentinel node; PET/CT; ^{89}Zr; Nanocoll; head and neck cancer

J Nucl Med 2013; 54:585–589
DOI: 10.2967/jnumed.112.115188

Sentinel nodes (SNs) near a primary tumor can be hidden by the high amount of radioactivity at the injection site. In such cases, the resolution of planar lymphoscintigraphy and SPECT/CT is limited (*1*). For oral cancer, this is especially true for tumors located in the floor of the mouth that drain to lingual lymph nodes or level I lymph nodes (*2,3*), which may explain the significantly lower sensitivity of the SN procedure for floor-of-mouth tumors than for other sites in the oral cavity (80% vs. 97%) (*4*).

PET provides dynamic 3-dimensional information at a higher spatial resolution and, thus, improves anatomic localization—of particular importance in the complex anatomy of the neck, with its abundant lymph nodes (i.e., about 150 on each side). In addition, improved visualization of lymphatic vessels may result in better differentiation between first- and second-echelon lymph nodes. Therefore, we hypothesized that PET might perform better than γ-camera–based techniques.

Recently, we developed ^{89}Zr-nanocolloidal albumin for lymphatic mapping and SN detection using PET/CT. The potential of this tracer was shown preclinically in a rabbit lymphogenic metastasis model (*5*).

The present study aimed to evaluate the feasibility of PET/CT lymphoscintigraphy using ^{89}Zr-nanocolloidal albumin in patients with early-stage oral cavity carcinoma and to obtain initial clinical experience in a head-to-head comparison with γ-camera–based imaging using ^{99m}Tc-nanocolloidal albumin.

MATERIALS AND METHODS

Patients

The study included 5 previously untreated patients with early-stage oral cancer who were scheduled for transoral excision and the SN procedure. Each patient had a clinically negative neck as assessed by ultrasound-guided fine-needle aspiration cytology. Three of the patients had a paramedian floor-of-mouth carcinoma, and 2 had a lateral tongue carcinoma. The study was approved by the Medical Ethics Committee of the VU University Medical Center and the National Competent Authority. All patients gave written informed consent before inclusion.

Preparation of ^{89}Zr- and ^{99m}Tc-Nanocolloidal Albumin

^{89}Zr (955 ± 167 MBq/mL; half-life, 78.4 h) was provided by BV Cyclotron VU. ^{89}Zr was conjugated to nanocolloidal albumin (Nanocoll; GE Healthcare) as described previously (*5*). In short, nanocolloidal albumin was first premodified with

Received Oct. 4, 2012; revision accepted Oct. 10, 2012.
For correspondence or reprints contact: Remco de Bree, Department of Otolaryngology/Head and Neck Surgery, VU University Medical Center, De Boelelaan 1117, P.O. Box 7057, 1007 MB Amsterdam, The Netherlands.
E-mail: r.bree@vumc.nl
Published online Feb. 1, 2013.
COPYRIGHT © 2013 by the Society of Nuclear Medicine and Molecular Imaging, Inc.

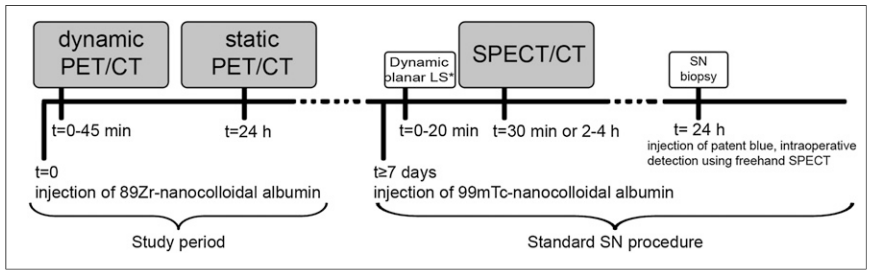

FIGURE 1. Time schedule of study events in relation to standard SN procedure.

p-isothiocyanatobenzyldesferrioxamine B (Macrocyclics), whereafter labeling with ^{89}Zr was possible. After 60 min of labeling, free ^{89}Zr was removed by size-exclusion chromatography using a PD10 column (GE Healthcare). The mean labeling efficiency was 63.6% ± 2.9%. ^{89}Zr-nanocolloidal albumin was filter-sterilized. These procedures resulted in a sterile final product of less than 2.5 endotoxin units/mL. The radiochemical purity was 96.9% ± 0.8%. ^{99m}Tc-nanocolloidal albumin was prepared according to the manufacturer's information (*6*).

Study Design

The study protocol (Fig. 1) consisted of 2 PET/CT scans after injection of 2.0 ± 0.8 MBq of ^{89}Zr-nanocolloidal albumin (divided into 4 peritumoral injections of 0.1 mL each). The first PET/CT scan (Gemini TF64; Philips Healthcare) consisted of 3 dynamic frames of 15 min each and was started almost directly after injection (+3–5 min). A second PET/CT scan (1 frame of 30 min) was obtained 24.4 ± 3.1 h after injection of ^{89}Zr-nanocolloidal albumin.

Seven to 9 d after the administration of ^{89}Zr-nanocolloidal albumin, the routine SN procedure was performed according to the guidelines of the European Association of Nuclear Medicine and the Sentinel European Node Trial Committee (*7*). In the 24 h before surgery, 100 MBq of ^{99m}Tc-nanocolloidal albumin were injected in a way similar to that for the ^{89}Zr-nanocolloidal albumin. Before injection, a scan was obtained to exclude retention of previously injected ^{89}Zr, and this prescan demonstrated that the influence of ^{89}Zr was negligible during the routine SN procedure.

Lymphoscintigraphic imaging consisted of dynamic planar imaging (20 frames of 60 s, 128 × 128 matrix, low-energy high-resolution

TABLE 1
Results of PET/CT and of Routine SN Procedure

Patient	Tumor	Level of foci identified on PET/CT	Level of foci identified on planar lymphoscintigraphy and SPECT/CT	SN biopsy	Blue	Pathology
1	T1 floor of mouth (paramedian R)	1× IB R (SN)	Not visible	Not detected		
		1× IB R (SN)	Not visible	Not detected	−	−
		2× II R (SN)	2× II R (SN)	2× II R	−	−
		1× III R (SN)	1× III R (SN)	1× III R		
2	T1 lateral tongue (R)	2× II R (SN)	2× II R (SN)	2× II R	+ (1×)	+ (1×)
		1× II R (second echelon)	1× II R (second echelon)	1× III R	−	−
		1× III R (second echelon)	1× III R (SN)			
3	T1 lateral tongue (L)	1× IB L (SN)	1× IB L (SN)	1x IB L	+	−
		1× II L (SN)	1× II L (SN)	1x II L	+	−
		1× II L (second echelon)	1× II L (second echelon)			
		1× III L (second echelon)	1× III L (second echelon)			
4	T2 floor of mouth (midline)	1× IB L (SN)	1× IB L (SN)	Not detected		
		2× II L (SN)	2× II L (SN)	2x II L	−	−
		1× III L (SN)	1× III L (SN)	1x III L	−	+
		1× IV L (second echelon)	1× IV L (second echelon)	1x IB R	−	−
		1× IB R (SN)	1× IB R (SN)			
		1× II R (second echelon)	1× II R (second echelon)			
		1× III R (second echelon)	1× III R (second echelon)			
		1× IV R (second echelon)	1× IV R (second echelon)			
5	T1 floor of mouth (paramedian R)	1× lingual node L (SN)	Not visible	Not detected		
		1× lingual node R (SN)	Not visible	Not detected	+	−
		1× IB R (SN)	Not visible	Not detected	−	−
		1× II L (SN)	1× II L (SN)	1x IB L		
		1× III L (SN)	1× III L (SN)	1x III L		
Total		27 (19 SNs)	22 (15 SNs)	14/15 (93%)	4/14 (29%)	

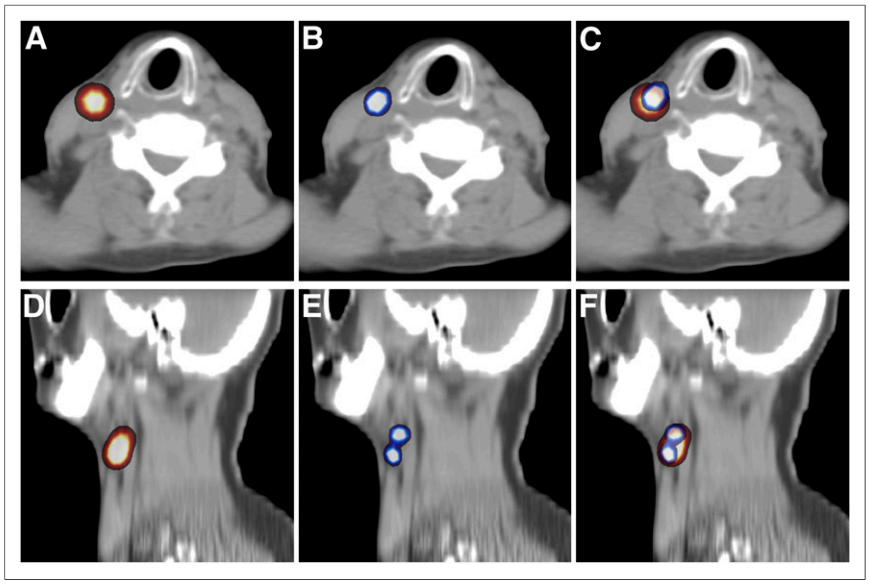

FIGURE 2. (A) SPECT/CT image of patient 1 demonstrating SN in level II of neck. (B) PET/CT image of same patient in which again SN in level II of neck was identified. (C) Fused SPECT and PET/CT image demonstrating uptake in exactly the same lymph node. (D) SPECT/CT image of patient 2, in whom 1 SN was identified (which was 2 hot spots on planar lymphoscintigraphy). (E) PET/CT image of patient 2 clearly showed 2 SNs. (F) Fused SPECT and PET/CT image again demonstrating identical drainage.

collimator, e.cam dual-detector camera; Siemens Medical Solutions) with the patients supine and the tumor side facing the camera, directly after the injection of ^{99m}Tc-nanocolloidal albumin. SPECT/CT (SymbiaT2; Siemens) was performed after 30 min (tongue carcinomas) or 2–4 h (floor-of-mouth carcinomas) (*8*). The SPECT/CT images were reconstructed by 2-dimensional ordered-subsets expectation maximization, with 4 subsets and 4 iterations and using segmented CT images for attenuation correction. Finally, the location of the SN was marked on the skin with a ^{57}Co point-source marker and was confirmed with a 14-mm-diameter conventional handheld γ-probe (Europrobe II; Eurorad). All injections were performed by the same person.

SN Biopsy Procedure

At the start of surgery (21.2 ± 1.8 h after injection of ^{99m}Tc-nanocolloidal albumin), 1 mL of patent blue V dye, diluted 1:3 (v/v) in water, was injected at 4 equally spaced points to completely surround the tumor. Subsequently, the SN was detected by means of the blue staining or with a freehand SPECT system that enabled intraoperative visualization of the SN and 3-dimensional navigation (Declipse SPECT; SurgicEye GmbHy) (*9*). Detected SNs were harvested and sent for histopathologic analysis. When the SN was metastatic, neck dissection was performed.

Image Analysis

The results of PET/CT and SPECT/CT were compared with respect to the total number and location of foci and, if visible, connecting lymphatic vessels. For comparison of different images, images were coregistered on the basis of low-dose CT using Vinci software (version 2.36.0; Max-Planck-Institut für Neurologische Forschung). All imaging results were analyzed by 3 different experienced persons. The location of the foci was classified into 1 of the 6 different lymph node levels in the neck according to the system of the American Academy of Otolaryngology–Head and

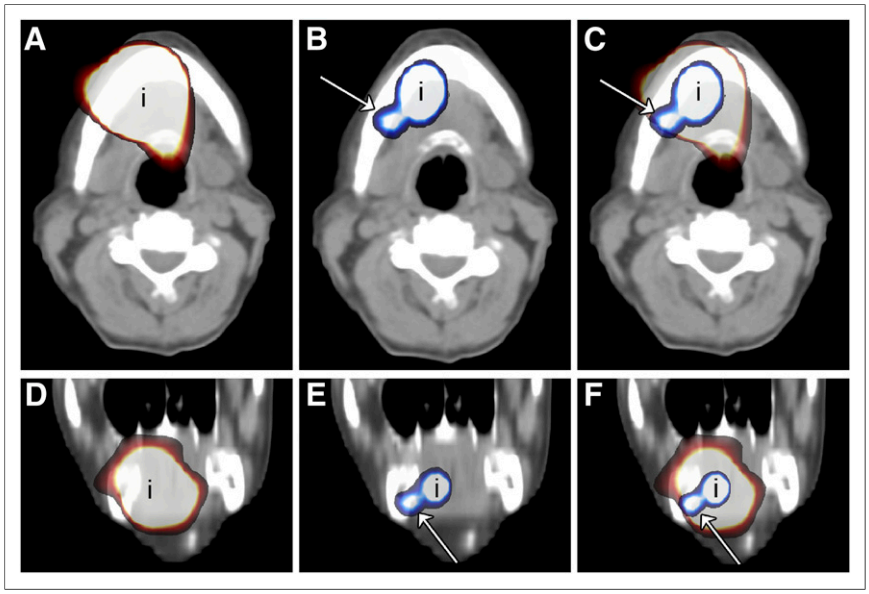

FIGURE 3. (A and D) Transversal (A) and coronal (D) SPECT/CT image of injection site (i) of patient 1, i.e., floor of mouth, in which only a large hot spot from injection site could be visualized. (B and E) PET/CT image of injection site of same patient in which level IB lymph node (arrow) clearly could be identified. (C and F) Fused SPECT and PET/CT images showing that lymph node visualized on PET/CT is hidden behind large hot spot on SPECT/CT images.

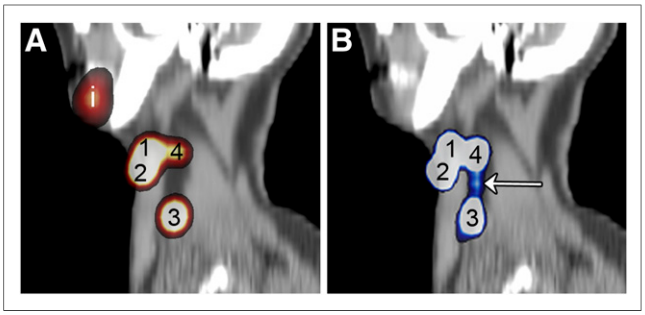

FIGURE 4. (A) Sagittal SPECT/CT image of patient 2, obtained 30 min after injection of ^{99m}Tc-nanocolloidal album, showed 4 hot spots of which 3 (1–3) were identified as SN and 1 (4) was identified as second-echelon lymph node due to lower uptake in this lymph node. (B) Sagittal PET/CT scan image of same patient in which same draining lymph nodes could be visualized. On this image (frame 3 of dynamic scan, i.e., obtained 30–45 min after injection of ^{89}Zr-nanocolloidal albumin), connecting lymphatic vessel (arrow) could be identified by increasing intensity of PET images, which clearly demonstrated that lymph node in level III (3) was also second-echelon lymph node instead of SN. i = injection site.

Neck Surgery (*10*). A focus was defined as a SN when tracer uptake was evident, and additional caudal foci with low uptake, not increasing in time, were considered to be second-echelon lymph nodes. A caudal focus with a clearly visible connecting lymphatic vessel from a cranial focus was also considered a second-echelon lymph node (*8*).

RESULTS

None of the patients experienced any adverse reaction from the administration of ^{89}Zr-nanocolloidal albumin. The effective dose equivalent of ^{89}Zr was 0.06 mSv (calculated using OLINDA software) with the injection of 2.0 ± 0.8 MBq of ^{89}Zr-nanocolloidal albumin.

The results of the SN procedure, including the results of the PET/CT scans, are presented in Table 1. In the 5 patients, a total of 22 foci were visualized on preoperative SPECT/CT images, of which 15 foci were considered to be SNs. The same 22 foci were also identified on PET/CT images (Fig. 2), and all foci identified on the first PET/CT scan were also identified on the second PET/CT scan. Moreover, in 2 patients, PET/CT was able to visualize 5 additional foci considered to be SNs (Table 1), all of which were near the primary floor-of-mouth tumor. On SPECT/CT, these foci were hidden by the hot spot at the injection site (Fig. 3). In 4 patients, lymphatic vessels could be visualized in the early phase of the dynamic PET/CT scan, and in 1 patient this visualization led to a better differentiation between a true SN and a second-echelon lymph node, compared with the SPECT/CT results (Fig. 4).

During surgery, 14 of 15 SNs identified with SPECT/CT could be harvested, of which 4 of 14 (29%) were both radioactive and blue. An SN in level Ib (floor-of-mouth tumor) and the additionally visualized PET foci near the primary tumor could not be detected intraoperatively. Histopathologic examination revealed 2 micrometastases in 2 patients, and both patients underwent neck dissection. No additional metastases were found in the surgical specimens.

DISCUSSION

In the present study, we demonstrated the feasibility of performing PET/CT lymphoscintigraphy using ^{89}Zr-nanocolloidal albumin in oral cancer patients. Lymphatic drainage patterns with ^{89}Zr-nanocolloidal albumin were identical to those with ^{99m}Tc-nanocolloidal albumin, with improved visualization of foci near the primary tumor site. Foci identified on the dynamic PET/CT scan were still visible during the second PET/CT scan, as is similar to the results obtained with ^{99m}Tc-nanocolloidal albumin in SPECT/CT. This finding demonstrates that ^{89}Zr-nanocolloidal albumin has excellent performance irrespective of whether it is used in a 1-d or a 2-d SN protocol.

Preoperative failure in SN detection is associated with a higher rate of intraoperative failure (*2*), and this observation makes preoperative identification an important factor in the SN procedure. Because PET/CT identified foci near the primary tumor, the next challenge is to improve intraoperative detection of these foci containing the positron emitter ^{89}Zr. Several options have to be considered. First, detection may be achieved using a handheld PET probe especially dedicated for detection of the 511-keV γ-rays emitted in the annihilation of an electron (e^-) and the positron (β^+). For sensitive detection, however, a large collimated and shielded detector is needed, making these probes heavy and not optimally suited for minimally invasive surgery. In addition, high-energy photons travel a long distance in soft tissue; therefore, such a probe will experience difficulties in differentiating between the SN and the injection site if they are near each other. That is less of a problem when one uses a β-probe, which can detect the β^+-particles. These particles have a short range, that is, a few millimeters in soft tissue, and thus particles arising from the injection site will not reach the detector. Because a β-probe needs a minimally collimated and shielded detector, it is suitable for minimal invasive use (*11*). Because of the short range of the β^+-particles, however, detailed preoperative anatomic localization is a prerequisite, which may be provided by PET/CT. Another promising approach for intraoperative detection is the use of near-infrared fluorescence imaging, which should also be able to identify SNs near the injection site (*12–14*). The different techniques have to be clinically evaluated in order to conclude which is best suited for intraoperative SN detection.

Lymphatic drainage of oral tumors is complex, with more than a single SN often being identified. Dynamic 2-dimensional planar lymphoscintigraphy and SPECT/CT are generally unable to visualize connecting lymphatic vessels. Because of this lack of clear visualization of lymphatic vessels, it is often difficult to decide whether a focus is a true SN or a second-echelon lymph node, especially for foci visualized late during lymphoscintigraphic imaging (*8*) as is often done with SPECT/CT. PET/CT was able to visualize lymphatic vessels in 4 patients. As a result, 1 focus

could be identified as a second-echelon node instead of an SN—a determination that was not possible on SPECT/CT (Fig. 4). Therefore, on the basis of the PET/CT findings, biopsy of this focus could be omitted, making the SN procedure as minimally invasive as possible.

CONCLUSION

PET/CT lymphoscintigraphy using ^{89}Zr-nanocolloidal albumin is feasible, with additional foci detected near the primary tumor site and more detailed localization of the foci. These preliminary results justify evaluation of ^{89}Zr-nanocolloidal albumin in more extensive comparative studies.

DISCLOSURE

The costs of publication of this article were defrayed in part by the payment of page charges. Therefore, and solely to indicate this fact, this article is hereby marked "advertisement" in accordance with 18 USC section 1734. This project was financially supported by Cancer Center Amsterdam VUmc Foundation. No other potential conflict of interest relevant to this article was reported.

ACKNOWLEDGMENTS

We thank Marijke Stigter-van Walsum (Otolaryngology/Head and Neck Surgery, VU University Medical Center) for helping to prepare the clinical-grade ^{89}Zr-nanocolloidal albumin. Furthermore, we thank Henri Greuter (Nuclear Medicine and PET Research) and Ellie Kemper (Clinical Pharmacology and Pharmacy, VU University Medical Center) for assistance during SN procedures.

REFERENCES

1. Haerle SK, Hany TF, Strobel K, Sidler D, Stoeckli SJ. Is there additional value of SPECT/CT over planar lymphoscintigraphy for sentinel node mapping in oral/oropharyngeal squamous cell carcinoma? *Ann Surg Oncol*. 2009;16:3118–3124.
2. Hornstra MT, Alkureishi LWT, Ross GL, Shoaib T, Soutar DS. Predictive factors for failure to identify sentinel nodes in head and neck squamous cell carcinoma. *Head Neck*. 2008;30:858–862.
3. Shoaib T, Soutar DS, MacDonald DG, Gray HW, Ross GL. The nodal neck level of sentinel lymph nodes in mucosal head and neck cancer. *Br J Plast Surg*. 2005;58:790–794.
4. Alkureishi LWT, Ross GL, Shoaib T, et al. Sentinel node biopsy in head and neck squamous cell cancer: 5-year follow-up of a European multicenter trial. *Ann Surg Oncol*. 2010;17:2459–2464.
5. Heuveling DA, Visser GWM, Baclayon M, et al. ^{89}Zr-nanocolloidal albumin-based PET/CT lymphoscintigraphy for sentinel node detection in head and neck cancer: preclinical results. *J Nucl Med*. 2011;52:1580–1584.
6. GE Healthcare. *Summary of Product Characteristics: Nanocoll*. Eindhoven, The Netherlands: GE Healthcare; August 2010.
7. Alkureishi LWT, Burak Z, Alvarez JA, et al. Joint practice guidelines for radionuclide lymphoscintigraphy for sentinel node localization in oral/oropharyngeal squamous cell carcinoma. *Eur J Nucl Med Mol Imaging*. 2009;36:1915–1936.
8. Heuveling DA, Flach GB, Van Schie A, et al. Visualisation of the sentinel node in early stage oral cancer: limited value of late static lymphoscintigraphy. *Nucl Med Commun*. 2012;33:1065–1069.
9. Heuveling DA, Karagozoglu KH, Van Schie A, Van Weert S, Van Lingen A, De Bree R. Sentinel node biopsy using 3D lymphatic mapping by freehand SPECT in early stage oral cancer: a new technique. *Clin Otolaryngol*. 2012;37:89–90.
10. Robbins KT, Clayman G, Levine PA, et al. Neck dissection classification update: revisions proposed by the American Head and Neck Society and the American Academy of Otolaryngology–Head and Neck Surgery. *Arch Otolaryngol Head Neck Surg*. 2002;128:751–758.
11. Heller S, Zanzonico P. Nuclear probes and intraoperative gamma cameras. *Semin Nucl Med*. 2011;41:166–181.
12. van den Berg NS, Brouwer OR, Klop WMC, et al. Concomitant radio- and fluorescence-guided sentinel lymph node biopsy in squamous cell carcinoma of the oral cavity using ICG-^{99m}Tc-nanocolloid. *Eur J Nucl Med Mol Imaging*. 2012;39:1128–1136.
13. Heuveling DA, Visser GWM, De Groot M, et al. Nanocolloidal albumin-IRDye 800CW: a near-infrared fluorescent tracer with optimal retention in the sentinel lymph node. *Eur J Nucl Med Mol Imaging*. 2012;39:1161–1168.
14. Bredell MG. Sentinel lymph node mapping by indocyanin green fluorescence imaging in oropharyngeal cancer: preliminary experience. *Head Neck Oncol*. 2010;2:31.